SPACE TELESCOPE SCIENCE INSTITUTE
Operated for NASA by AURA

Instrument Science Report STIS 2004-01

A New Geometric-Distortion Solution for the STIS NUV-MAMA

J. Maíz-Apellániz & L. Úbeda
March 1, 2004

ABSTRACT

We have obtained a new geometric-distortion solution for the STIS NUV-MAMA using two fields in NGC 4214 and NGC 604 which were imaged using three filters (CN182, CN270, SrF2) for GO program 9096. (WF)PC2 images of the same objects in F170W and F336W were used as an astrometric reference. Different polynomial degrees and weighting mechanisms for the geometric distortion were tested until an adequate solution was obtained. Typical median errors between the predicted and the real positions were found to be in the range of 0.28 to 0.53 MAMA pixels (7-13 mas). A new geometric distortion table has been produced and tested. We discuss differences between this solution and the previous one that was presented in STIS Instrument Science Report 2001-02.

Introduction

While developing a software tool for the analysis of objective-prism data obtained with the STIS NUV-MAMA, we discovered that the current implementation of the geometric distortion solution was incorrect. Apparently, the error originated in a different assumed shape for the output pixels between the solution developed by Walsh et al. (2001) and its implementation in the IDCTAB reference table. Walsh et al. (2001) assumed rectangular pixels (i.e. different x and y sizes) while IDCTAB assumed square ones (i.e. same size in x and y). As a result, the errors in the corrected positions are as large as ~5 pixels.

The NUV-MAMA objective-prism data we had obtained consists of three different fields, one of them in the Giant H II Region NGC 604 and two in the nearby galaxy NGC

Copyright© 1999 The Association of Universities for Research in Astronomy, Inc. All Rights Reserved.

4214. Each field was imaged using two different orientations, and each one of the orientations has two exposures with a small spatial displacement between them. The objective-prism data was complemented with short imaging exposures using the same NUV-MAMA detector in order to find the positions of the sources in the main exposures. Here we will use some of those images for the purpose of deriving a new geometric distortion solution.

The technique used by Walsh et al. (2001) involved taking multiple exposures of the same field with small displacements between them but with the same orientation and guide stars and involves no previous knowledge of the positions of the stars in the field. This method has the drawback that the skewing terms in the distortion solution cannot be constrained (Anderson & King 2003). Here we will use a different approach. One of the NGC 4214 fields has been imaged with the PC of the WFPC2 using F170W and F336W using two orientations which differ by almost 180^{o} from one another (see Fig.1) while the NGC 604 field has been imaged with the PC using F170W and a single orientation. Given that we had data in the same wavelength range obtained with an instrument with an accurate geometric distortion solution (Anderson & King 2003, Kozhurina-Platais et al. 2003), we decided to measure the positions of the stars in the PC images, correct the geometric distortion there, and use those 'real' positions to generate an 'astrometric flat field'. Then the positions of the same stars could be measured in the NUV-MAMA images and the geometric-distortion solution calculated directly using the difference between the measured and the real positions. This is the same idea which was used recently by Kozhurina-Platais et al. (2003) to produce a multi-wavelength geometric distortion solution for the WFPC2. Those authors used F555W positions to generate the astrometric flat field and then measured the positions of the same stars in other filters.

Data

The STIS and WFPC2 data sets used in this work are listed in Tables 1 and 2 respectively. All STIS datasets were obtained for GO program 9096 (P.I.: Maíz-Apellániz). The NGC 4214 WFPC2 data sets were obtained for GO program 6716 (P.I.: Stecher) and the NGC 604 WFPC2 data sets were obtained for GO program 5384 (P.I.: Waller).

Table 1. STIS data sets used.

field/orientation	CN182	CN270	SrF2
NGC4214/1	o6bz02isq, iwq	o6bz02j7q, jbq	
NGC 4214/2	o6bz01afq		
NGC 604/1			o6bz06wuq
NGC 604/2	o6bz05p7q		

Table 2. WFPC2 data sets used.

field/orientation	F170W	F336W
NGC4214/1	u4190101r,02r	u4190103r,04r
NGC 4214/2	u4190201m,02m	u4190203m,04m
NGC 604	u2c60b01t, 02t	

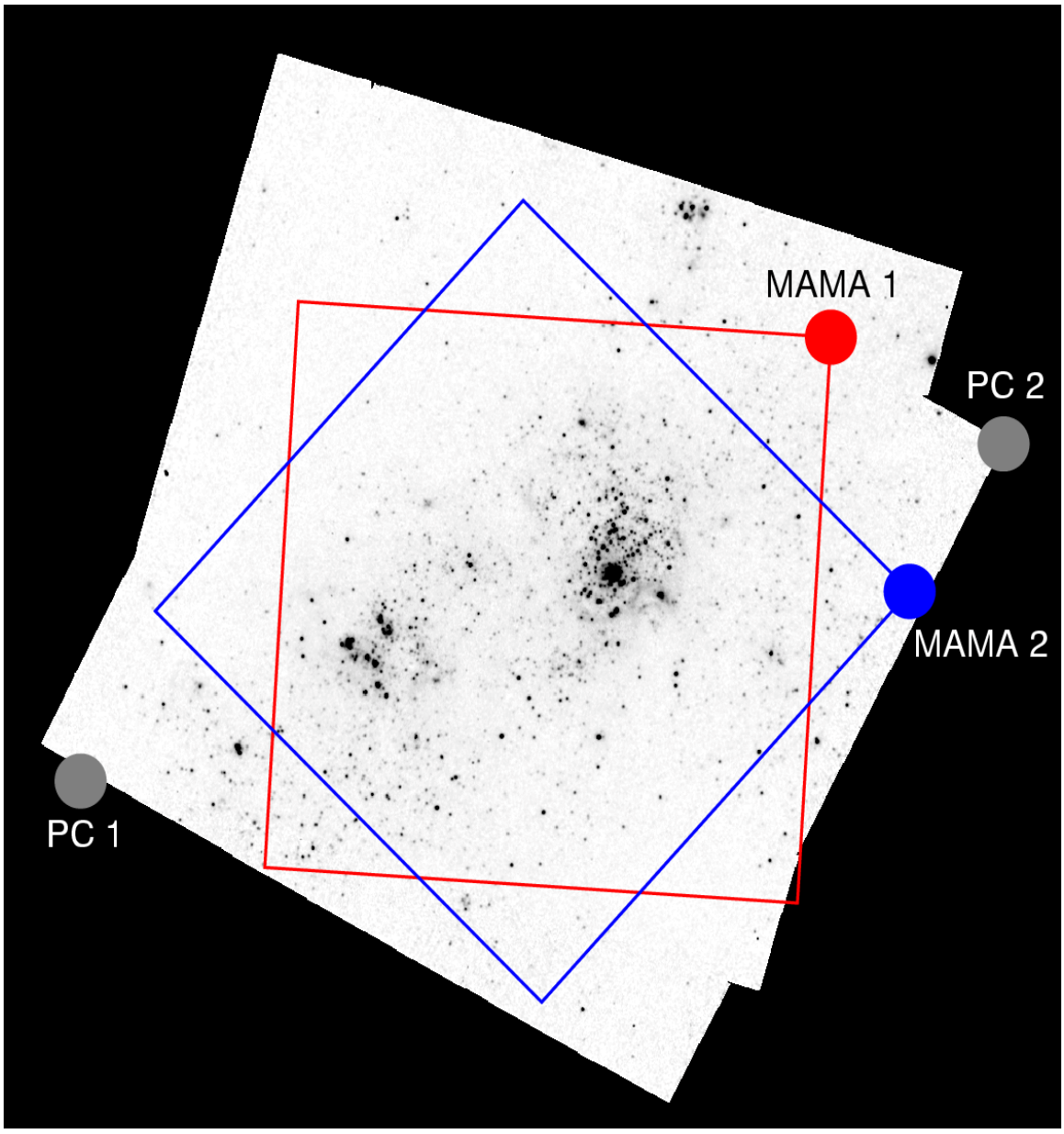

Figure 1: Mosaic of the two F336W NGC 4214 PC orientations with the outline of the two corresponding MAMA orientations overimposed. Circles indicate the lower left corner of the detector for each of the four orientations.

Six additional STIS data sets (three for NGC 4214 and three for NGC 604) were not used due to the anomalous PSFs caused by breathing.

Analysis

WFPC2 data

PSF-fitting photometry was performed using HSTphot (Dolphin 2000) for each of the five field/orientation/filter combinations in Table 2. HSTphot is a crowded-field photometry program written in C which is tailored to the specific characteristics of the WFPC2 instrument. Normally, HSTphot is used for multiple-filter data and the output is placed into an F555W-based coordinate system by applying the Holtzmann et al. (1995) geometric-distortion solution corrected for the different plate scale associated with each filter (Dolphin 2000, note that in the current version of HSTphot, 1.1, multiphot has been renamed to hstphot). For NGC 4214 we processed the F170W and F336W data for each of the two orientations independently rather than generating a single star list for each orientation (for NGC 604 we only used F170W data and one orientation). Then, the two star lists for each filter were combined by applying a shift which minimizes the measured distances between the position of the stars detected in the two orientations (this was needed due to the use of different guide stars for each orientation) and then using the mean of the two positions as the final value for each star. The final distance histogram is shown in Fig. 2 for F336W. Note that the value plotted is the distance between the two positions, so a reasonable estimate for the uncertainty between the measured and the real position would be one half of that amount. This leads to a typical uncertainty of 0.104 PC pixels = 4.7 mas, which coincides with the 5 mas precision expected from the Holtzmann et al. (1995) solution (Casertano & Wiggs 2001).

The number of stars detected in the PC data was 173 (NGC 4214, F170W), 1008 (NGC 4214, F336W), and 329 (NGC 604, F170W, here we discarded some close binaries, see Maíz-Apellániz et al. 2004). Most of the NGC 4214 F336W stars which are not present in the F170W list are expected to be UV-bright early-type stars which are not detected in the latter filter due to its low throughput. Given the better sensitivity in the UV of the NUV-MAMA, we would expect to detect some of those stars in our STIS data. Also, given the need for at least several hundred stars for adequate sampling when calculating a geometric distortion solution and the lack of any apparent systematic effect between the F170W and F336W positions in the NGC 4214 data, we decided to use only the latter as our reference for that field.

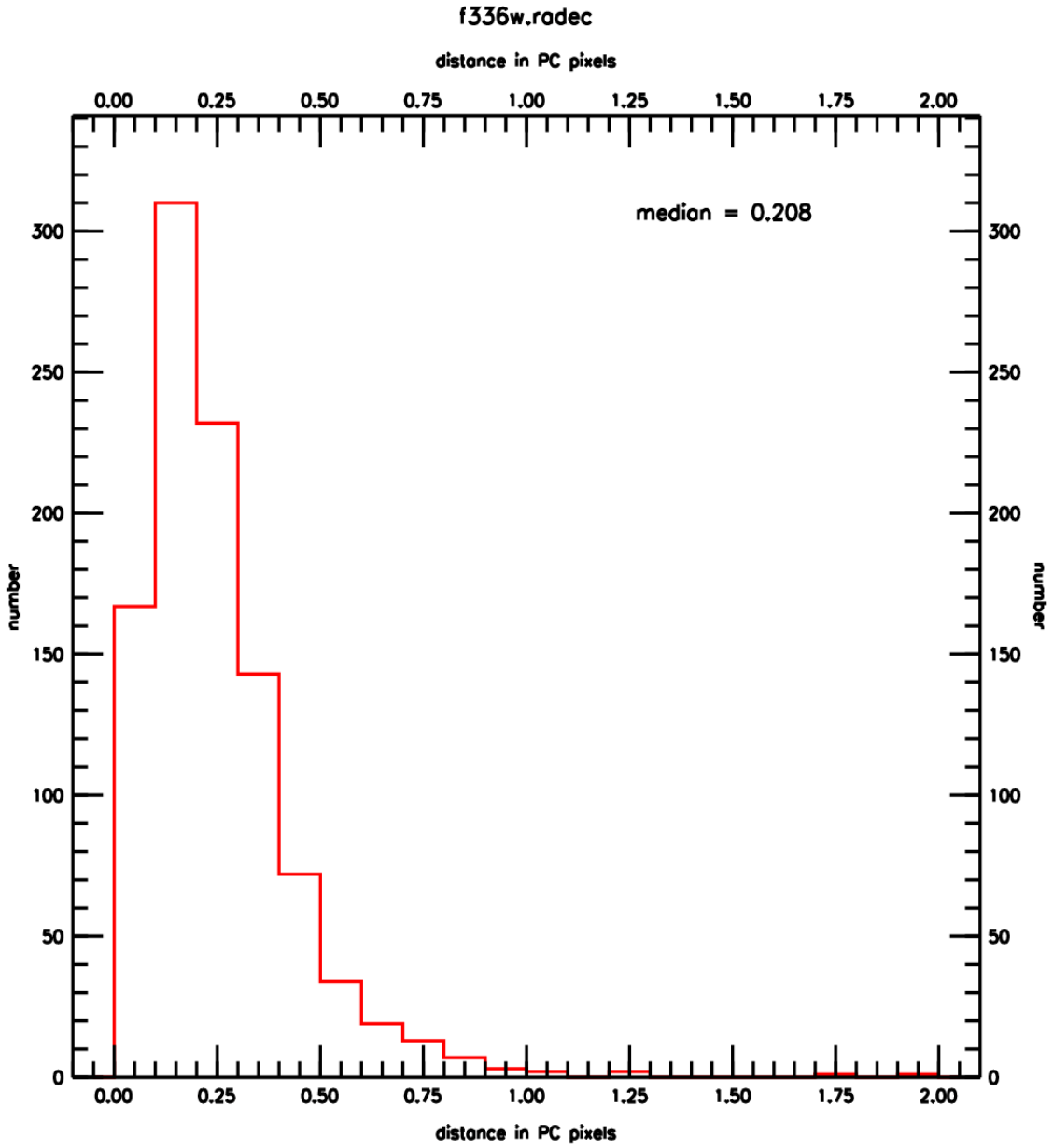

Figure 2: Histogram for distances between the two positions measured for stars detected in both F336W NGC 4214 PC orientations.

STIS data

In order to process the STIS data we wrote an IDL code which first translates the right ascension and declination of the positions in the WFPC2-generated list into the NUV-MAMA detector coordinate system. Using that coordinate list and an initial guess of the geometric distortion solution, the positions of the stars in the STIS images are first estimated and then measured using a centroiding algorithm. In a first pass, the code eliminates

stars with nearby companions or with low values of the S/N ratio and then calculates the displacement and possible rotation between the WFPC2 and the STIS coordinates. In its second pass it corrects for the displacement and rotation and assigns a weight to each star. Different weighting mechanisms were tested and we finally chose one in which stars with shorter distances between the positions measured in the two PC orientations had higher weights (low values for those distances should indicate, at least on average, a better precision for the input positions). For the NGC 604 data, where only one orientation was available, we simply gave a higher weight to the brighter stars (since a higher S/N ratio leads to smaller errors in the measured positions due to centroiding). After producing in this manner a list of input ('real') x_i, y_i and measured x, y positions, we are ready to calculate the geometric distortion model following the polynomial expressions defined by Hack & Cox (2000) for the IDCTAB table:

$$x_i - x_r = \sum_{i=0}^{k} \sum_{j=0}^{i} c_{x,i,j} (x - x_r)^j (y - y_r)^{i-j} \qquad (1)$$

$$y_i - y_r = \sum_{i=0}^{k} \sum_{j=0}^{i} c_{y,i,j} (x - x_r)^j (y - y_r)^{i-j} \qquad (2)$$

where x_r , y_r are the coordinates of a reference position in the center of the detector (in our case 512, 512), k is the polynomial degree and $c_{x,i,j}$, $c_{y,i,j}$ are the polynomial coefficients for the direct (measured to real) transformation. The corresponding inverse (real to measured) transformation is:

$$x - x_r = \sum_{i=0}^{k} \sum_{j=0}^{i} d_{x,i,j} (x_i - x_r)^j (y_i - y_r)^{i-j} \qquad (3)$$

$$y - y_r = \sum_{i=0}^{k} \sum_{j=0}^{i} d_{y,i,j} (x_i - x_r)^j (y_i - y_r)^{i-j} \qquad (4)$$

where $d_{x,i,j}$, $d_{y,i,j}$ are the polynomial coefficients. The four sets of polynomial coefficients were calculated using the IDL routine MPFIT2DFUN created by Craig Markwardt (avail-

able from http://cow.physics.edu/~craigm/idl/idl.html). In order to minimize round-off errors, a scale transformation that placed all coordinates in the range [-1,1] was applied prior to the calculation. The scale transformation was reversed after the coefficients were obtained.

An independent solution was obtained for each of the seven data sets listed in Table 1. Small variations were observed between each one of them, which could in principle be real (i.e. due to filter or temporal dependencies) or caused by sampling effects (each field and orientation had a different and non-uniform coverage of the detector, as is readily apparent from e.g. Fig. 1). In order to test this, we produced two new solutions including the NGC 4214 data obtained either with the CN182 or the CN270 filters. No large variations were observed between them, suggesting that the dependence on wavelength of the solution is weak or inexistent (see also Table 4). The use of different filters and a short baseline between observations precluded the accurate testing of a possible temporal evolution. Therefore, lacking a more complete information, we simply decided to produce one final solution including the positions from all seven data sets, since this strategy should minimize errors produced by inadequate sampling present in the individual solutions for the seven data sets.

We also tested whether changing *k* had an effect or not in the precision of our solution. We tried values of 3, 4, and 5 and the results are shown in Figure 3 in the form of the median distance between the PC and MAMA coordinates for the stars in each of the seven data sets using the final solution discussed in the previous paragraph. Only small variations are seen between the three values of the polynomial degree, indicating that a value as low as k=3 yields a reasonable correction. Six of the seven data sets are better fitted with a fourth degree polynomial than with a third degree one but increasing *k* to five yields no significant improvement (in three cases the median distance actually increases). Therefore, we adopted a fourth degree polynomial for our final solution.

The median precision for the five NGC 4214 data sets is 0.28-0.42 MAMA pixels (7-10 mas) while that of the two NGC 604 data sets is 0.50-0.53 MAMA pixels (12-13 mas). The fact that the NGC 604 reference positions were measured using only one PC orientation while those of NGC 4214 were measured with two seems to indicate that part of the error budget resides in the Holtzmann et al. (1995) solution for the PC. This is not unexpected, given its estimated precision of 5 mas.

Implementation

We have produced a new IDCTAB table, nas13578o_idc.fits, which was implemented in the pipeline on 29 October 2003. The values for the polynomial coefficients are shown in Table 3. The distortion map is shown in Figure 4. Note that the values in Table 3 are defined by Eqns. (1-4), which transform from pixel coordinates into pixel cordinates. The equivalent coefficients for the IDCTAB table transform from pixels to arcseconds for the

direct transformation (Eqns. 1 and 2) and from arcseconds to pixels for the inverse one (Eqns. 3 and 4). The mean scale used for the conversion was 24.6775 mas/pixel (note that this value is somewhat arbitrary since, in principle, one could use a slightly different scale and change the number of pixels in the output image in each direction by a few).

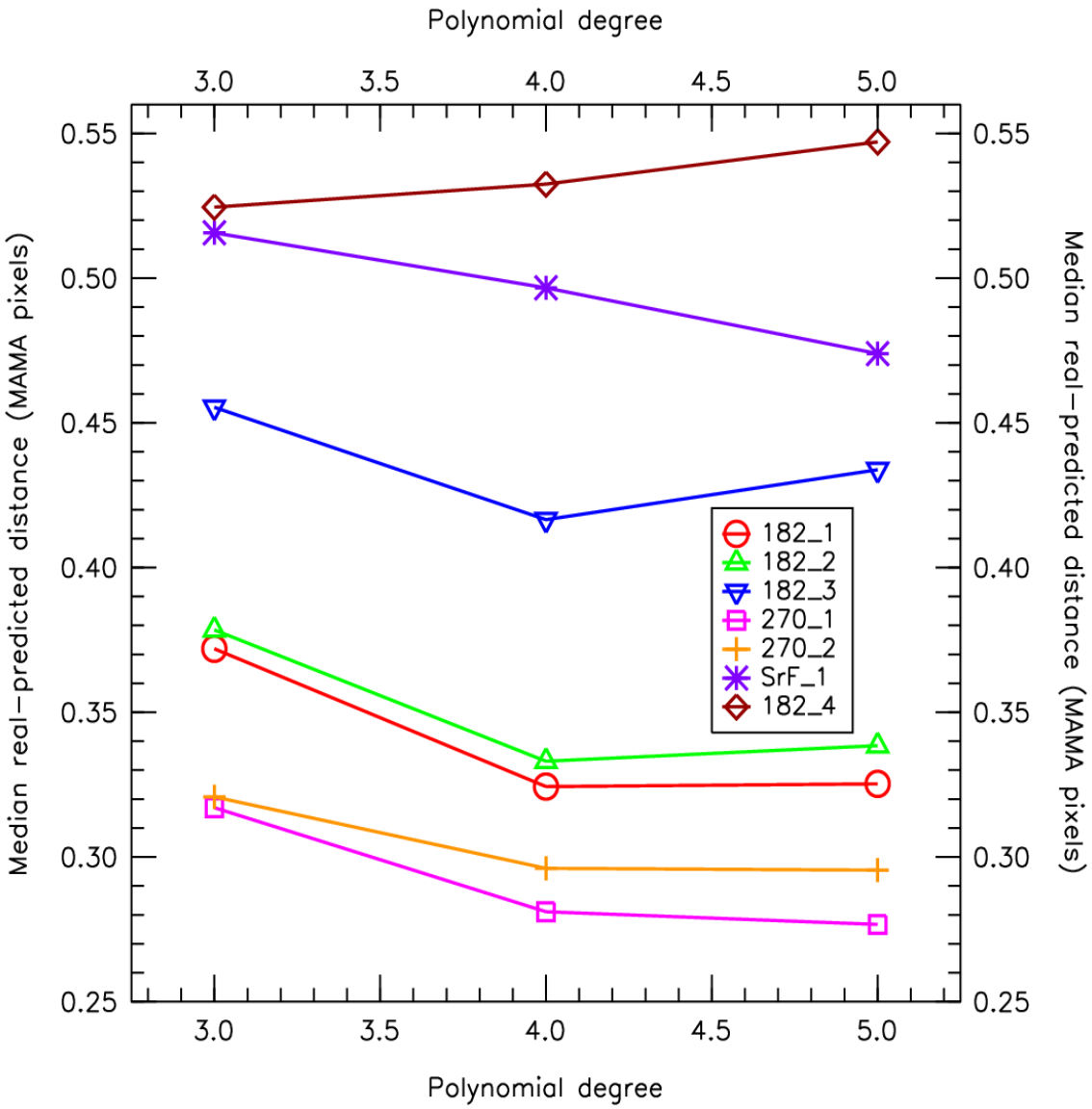

Figure 3: Median value for the distance between the PC-based position and the MAMA-measured one (including the geometric distortion solution) for the stars detected in each of the seven MAMA fields used (the first five are for NGC 4214 data and the last two for NGC 604) as a function of polynomial degree.

Table 3. Polynomial coefficients.

i	j	c_x	c_y	d_x	d_y
0	0	0.00000000000E+00	0.00000000000E+00	0.00000000000E+00	0.00000000000E+00
1	0	-9.46260769040E-04	1.00169217898E+00	9.72669788803E-04	9.98323338813E-01
1	1	9.89989681864E-01	-5.00637730808E-04	1.01013838297E+00	5.18851321984E-04
2	0	3.73428826165E-06	-1.37170502615E-06	-3.71684432187E-06	1.37070097018E-06
2	1	7.30367203585E-06	5.42519173844E-06	-7.47281028965E-06	-5.45923399495E-06
2	2	8.61203692686E-06	3.69010949295E-06	-8.92126636437E-06	-3.77754019541E-06
3	0	3.74484130169E-09	2.13371895424E-09	-3.82251104228E-09	-2.17377911461E-09
3	1	-4.10671509032E-09	-1.22689770675E-09	4.17191995209E-09	1.21018730090E-09
3	2	-1.59931588005E-09	-4.91316849689E-09	1.60884114888E-09	4.93440681977E-09
3	3	6.52790805981E-09	-1.18209732673E-09	-6.89366636304E-09	1.07518729483E-09
4	0	-5.17407045044E-12	5.47388163085E-13	4.98979456193E-12	-5.90413976340E-13
4	1	-1.35759604502E-11	4.05487186887E-12	1.38253979379E-11	-3.98844371489E-12
4	2	-6.89591843517E-12	1.37884434174E-12	7.03845436828E-12	-1.46646818742E-12
4	3	-6.79163498427E-12	-1.62340960474E-11	7.25822569205E-12	1.65327255853E-11
4	4	-1.21452689835E-11	-2.16275305786E-11	1.30975131835E-11	2.24614370453E-11

The previous IDCTAB table for the NUV MAMA was l8g1208go_idc.fits, and as we mentioned before, it did not provide an accurate geometric distortion solution (see Figure 5). Furthermore, the distortion map produced from the parameters there is different from Fig. 12 of Walsh et al. (2001). Either of those are also very different from our Figure 4. Apparently, some error must have been present in the previous calculations or implementations. As previously mentioned, a possibility is that the calculation implied the use of rectangular pixels and that this was neglected in the implementation, but even this does not explain the differences between the parameters in l8g1208go_idc.fits and Fig. 12 of Walsh et al. (2001). These problems preclude the comparison of the new solution with the previous one except in one aspect, the mean scales for *x* and *y*, which are shown in Table 4. We show there our final results, as well as that of Walsh et al. (2001), and the scales derived from our data independently for CN182 and CN270 using only the NGC 4214 field. As previously mentioned, no significant differences are seen among our three solutions since both the CN182 and CN270 ones are within 1 σ of the final solution for both the *x* and the *y* scales. Our final result for the scales is also easily compatible with the Walsh et al. (2001) one.

Table 4. Pixel scales.

	x scale (mas/pix)		y scale (mas/pix)	
NGC 4214, CN182	24.533	0.037	24.793	0.037
NGC 4214, CN270	24.541	0.037	24.831	0.037
Final	24.536	0.027	24.795	0.031
Walsh et al. (2001)	24.526	0.120	24.829	0.126

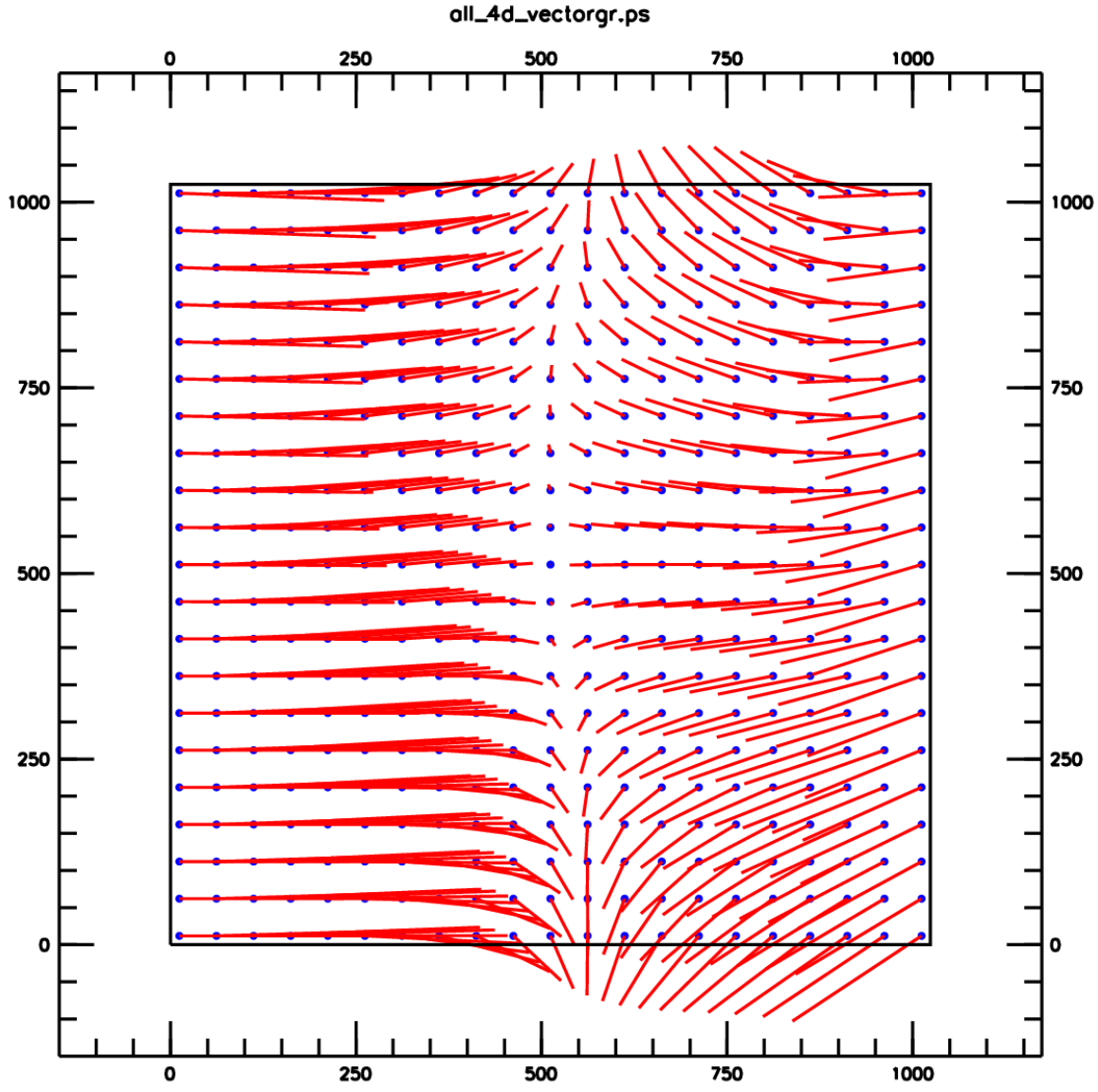

Figure 4: Distortion map for the NUV MAMA. Each vector represents the distortion in pixels magnified by 50. The dot shows the uncorrected position and the vector the correction to the geometrically correct position.

Future work

There are two ways in which this solution could be improved in the future. One would be to use as a reference the new improved geometric distortion solutions for the PC, which have RMS errors of only 1 mas in F555W (Anderson & King 2003) and 2 mas in F300W (Kozhurina-Platais et al. 2003), thus increasing the precision of the astrometric flat field. The second way would be to use a globular cluster field with observations deep enough to have several thousand stars in common between the PC and the STIS data, thus increasing the sampling across the detector. We also plan to improve the geometric distortion solutions of the STIS FUV-MAMA and CCD using a technique similar to the one in this ISR.

References

Anderson, J. & King, I. 2003. *An Improved Distortion Solution for the Hubble Space Telescope WFPC2*. PASP 115, 113.

Casertano, S. & Wiggs, M. S. 2001. *An improved geometric solution for WFPC2.* WFPC2 Instrument Science Report 2001-10.

Dolphin, A. E. 2000. *WFPC2 Stellar Photometry with HSTphot.* PASP 112, 1383.

Hack, W. & Cox, C. 2000. *Geometric Distortion Table: IDCTAB.* ACS Instrument Science Report 2000-11.

Holtzmann, J. et al. 1995. *The performance and calibration of WFPC2 data on the Hubble Space Telecope.* PASP 107, 156.

Kozhurina-Platais, V., Anderson, J., & Koekemoer, A. M. 2003. *Towards a Multi-Wavelength Geometric Distortion Solution for WFPC2.* WFPC2 Instrument Science Report 2003-02.

Maíz-Apellániz, J. et al. 2004. *NGC 604, the SOBA Prototype II - UV and Optical Photometry and UV Spectroscopy.* In preparation.

Walsh, J. R., Goudfrooij, P., & Malamuth, E. 2001. *STIS Geometric Distortion - SMOV3A tests for CCD, NUV-MAMA, and FUV-MAMA.* STIS Instrument Science Report 2001-02.

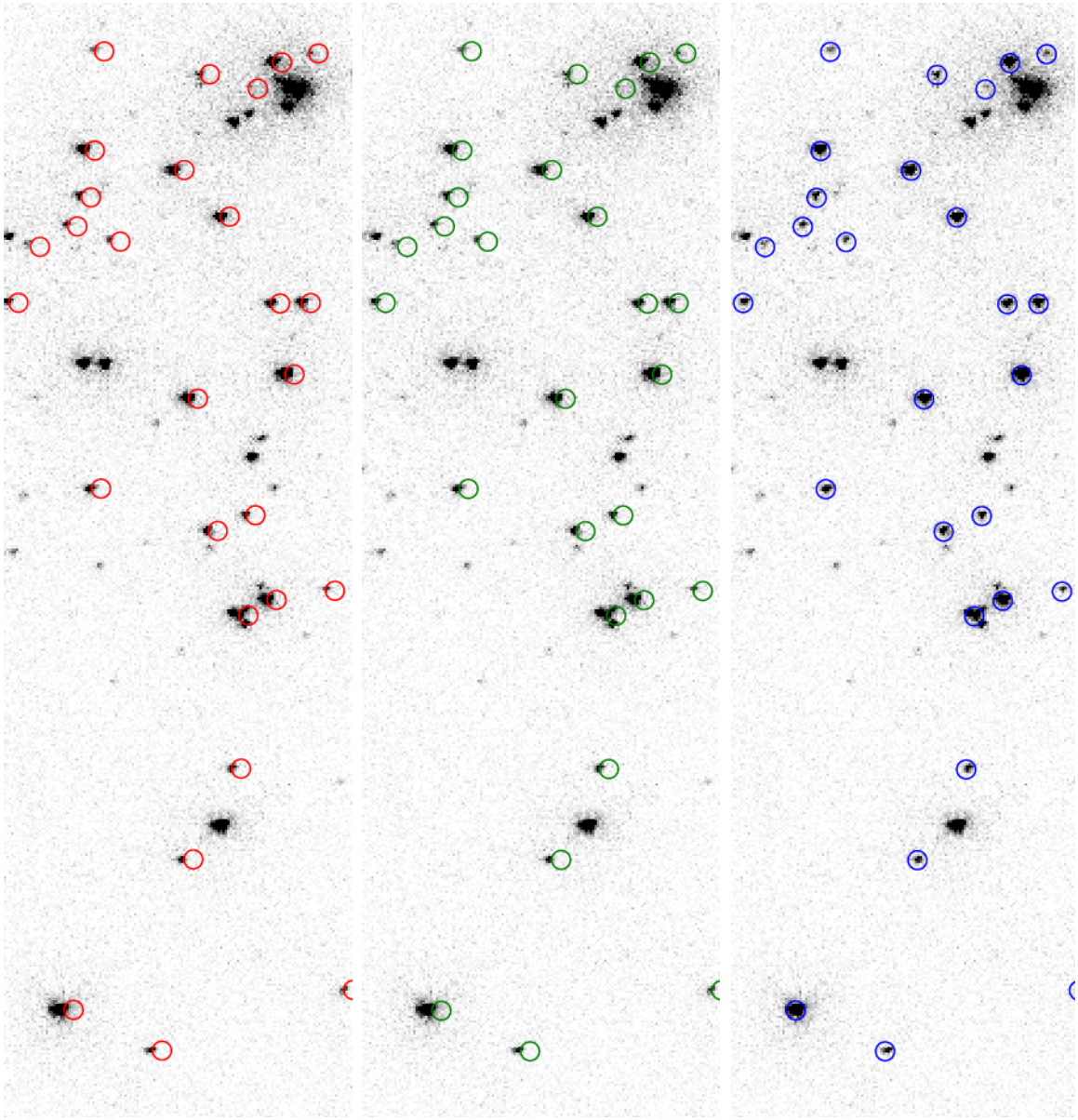

Figure 5: Section of the NGC 604 NUV MAMA SrF2 field with the positions of the stars (marked by circles) derived from the PC data with (left) no geometric distortion solution, (center) the solution from the IDCTAB file l8g1208go_idc.fits, and (right) the geometric distortion solution derived here. The section has a size of 154 x 513 pixels.